Pharmaceutical Research, Vol. 25, No. 7, July 2008 (© 2008)
DOI: 10.1007/s11095-008-9560-0

Research Paper

What is a Suitable Dissolution Method for Drug Nanoparticles?

Desmond Heng,[1,3] David J. Cutler,[1] Hak-Kim Chan,[1,4] Jimmy Yun,[3] and Judy A. Raper[2]

Received December 12, 2007; accepted February 19, 2008; published online March 5, 2008

Purpose. Many existing and new drugs fail to be fully utilized because of their limited bioavailability due to poor solubility in aqueous media. Given the emerging importance of using nanoparticles as a promising way to enhance the dissolution rate of these drugs, a method must be developed to adequately reflect the rate-change due to size reduction. At present, there is little published work examining the suitability of different dissolution apparatus for nanoparticles.
Methods. Four commonly-used methods (the paddle, rotating basket and flow-through cell from the US Pharmacopia, and a dialysis method) were employed to measure the dissolution rates of cefuroxime axetil as a model for nanodrug particles.
Results. Experimental rate ratios between the nanoparticles and their unprocessed form were 6.95, 1.57 and 1.00 for the flow-through, basket and paddle apparatus respectively. In comparison, the model-predicted value was 7.97. Dissolution via dialysis was rate-limited by the membrane.
Conclusions. The data showed the flow-through cell to be unequivocally the most robust dissolution method for the nanoparticulate system. Furthermore, the dissolution profiles conform closely to the classic Noyes–Whitney model, indicating that the increase in dissolution rate as particles become smaller results from the increase in surface area and solubility of the nanoparticles.

KEY WORDS: cefuroxime axetil; drug nanoparticles; Noyes–Whitney equation; poorly water-soluble drug; powder dissolution apparatus.

INTRODUCTION

The Noyes–Whitney and other related models (1–6) (Eqs. 1–3) infer a direct proportionality between the dissolution rate and the specific surface area of a powder.

$$\text{Classic Noyes} - \text{Whitney equation}: \frac{dM}{dt} = k(C_S - C) = k_1 \cdot S(C_S - C) \quad (1)$$

$$\text{Nernst} - \text{Brunner model}: \frac{dM}{dt} = S \cdot \frac{D}{h}(C_S - C) \quad (2)$$

$$\text{Danckwerts}' \text{ surface} - \text{renewal model}: \frac{dM}{dt} = S \cdot \sqrt{D \cdot p}(C_S - C) \quad (3)$$

where M is the mass of drug dissolved in time t, k and k_1 are constants, C_S is the saturation solubility of the solute, C the bulk concentration of the solute in the medium at time t, D the diffusion coefficient of the solute in the dissolution medium, S the specific surface area of the solids, h the stagnant layer thickness and p the mean rate of surface renewal, a quantity related to agitation or stirring (7).

For poorly soluble compounds, a variant form of Eq. 1 (with k_1 constant) has been proposed (8) which differs from the Nernst–Brunner equation (Eq. 2) by including a term to describe molecular dissociation from the surface as well as diffusion into the bulk media.

The increase of specific surface area with decreasing particle size offers the great potential of higher dissolution rates for these valuable drugs. Hence, particle size reduction techniques (e.g. micronization or nano-sizing) are crucial for realizing better bioavailability of drugs with poor dissolution (9). Current strategies for engineering drug nanoparticles include the use of supercritical fluids (10), aerosols (11), high-gravity reactive/antisolvent precipitation (12), microemulsification (13), and confined impinging jets (14).

The definition of a nanoparticle depends on the discipline (15,16). In colloid chemistry, particles are only classified as nanoparticles when they are <100 nm. However, obtaining sizes <100 nm is more readily achieved with hard materials (e.g. silica, metal oxides) than with softer materials such as drugs and polymers (16). Hence, in the pharmaceutical industry, a nanoparticle is more commonly defined as having a size between a few nanometers and 1 μm (based on the size

[1] Advanced Drug Delivery Group, Faculty of Pharmacy, A15, The University of Sydney, Sydney, NSW 2006, Australia.
[2] Department of Chemical Engineering, University of Missouri-Rolla, Rolla, Missouri 65409, USA.
[3] Nanomaterials Technology Pty. Ltd., 28 Ayer Rajah Crescent, #03-03, Singapore 139959, Singapore.
[4] To whom correspondence should be addressed. (e-mail: kimc@pharm.usyd.edu.au)

unit) (15). A reasonable size goal of around 300 nm has been proposed by Gupta (16) for drug and polymer materials, although the US FDA currently considers nanoparticles to be <100 nm in at least one dimension (17).

An increasing array of newly developed drugs in the pharmaceutical industry are poorly water-soluble, mainly due to the application of high throughput screening (HTS) techniques during the discovery and development process, which tend to bias towards the higher molecular weight and lipophilic compounds (18). For these compounds (i.e. these drugs usually fall into Class II of the Biopharmaceutics Classification Scheme (BCS) scheme—low-solubility, high-permeability compounds (19)), the dissolution rate is the limiting factor for the drug absorption rate (20).

Preliminary work by Finholt (1,21) on microparticles indicated that the wetting behaviour of a hydrophobic drug would be compromised with decreasing particle size, resulting in the inability to properly measure the dissolution rate. With nanoparticles, this property may be accentuated, hence sparking a need for a suitable dissolution method that can truly reflect the nanoparticle dissolution behaviour.

In relation to the dissolution models (Eqs. 1–3), the bulk concentration of the solute in the medium is much lower than its saturation solubility at the initial stages of dissolution. Hence, $(C_S - C) \approx C_S$. For a given dissolution apparatus, the solvent and flow conditions remain unchanged irrespective of the solute (i.e. same D, h, V, p). Therefore, the dissolution rate ratio of two solutes in a given dissolution apparatus, simplifies down to the product of their specific surface area and saturation solubility ratios. This simplification is common to all the three models.

$$\frac{\left(\frac{dM}{dt}\right)_{\text{nanoparticles}}}{\left(\frac{dM}{dt}\right)_{\text{unprocessed}}} = \frac{(S \cdot C_S)_{\text{nanoparticles}}}{(S \cdot C_S)_{\text{unprocessed}}} \tag{4}$$

In-vitro dissolution testing has become an important aspect of the drug development process, due to its ability to compare the performance of different formulations. Existing powder dissolution apparatus include the paddle, basket, flow-through method and the dialysis bag (22,23). Of particular versatility is the flow-through cell, demonstrated by its use in characterizing the biopharmaceutical qualities of powdered active ingredients (23), tablets (24), capsules (25), suppositories (26) and parenteral implants (i.e. intramuscular implants of controlled-release preparations) (27). This method is particularly favoured for the *in-vitro* dissolution of poorly water-soluble drugs (27,28) due to its ability to operate under sink conditions. No further filtration steps are needed, as any undissolved particles are kept within the cell (28). To the authors' knowledge, the suitability of this method for nanoparticles is still unknown. Previous comparative studies of different dissolution apparatus (i.e. USP and non-USP) focused mainly on tablets (24,29–31) and capsules (25,31,32). Only a few studies have dealt with active pharmaceutical ingredients (API) in the powdered form (23,33,34), and with limited scope, involving less than three apparatus. However, no detailed comparative studies have been performed for powdered drug nanoparticles.

In the absence of comparative data, researchers in pharmaceutical nanotechnology today still use the paddle apparatus in their dissolution experiments (9,35,36) despite evidence of potential unsuitability, e.g. the hydrodynamics of both the paddle and basket apparatus had previously been shown to be highly non-uniform, giving rise to fluctuations in the dissolution rate measurements (23,37).

In this paper, the suitability of the paddle, basket, flow-through cell and dialysis methods for nanoparticles was compared in relation to the dissolution models. Cefuroxime Axetil (CFA), a cephalosporin antibiotic (38), was used as the model drug due to its class II status (12,19), whereby the dissolution rate is the limiting factor towards much improved oral bioavailabilities.

MATERIALS AND METHODS

Preparation of CFA Nanoparticulate Powder

CFA nanoparticles were obtained using the High-Gravity Antisolvent Precipitation Method described previously by Chen *et al.* (12). Briefly, CFA raw powder (NCPC Beta Co. Ltd., China) was dissolved in acetone (10% *w/v*), and re-precipitated in a rotating packed bed reactor via the concurrent introduction of the CFA solution and an antisolvent stream of isopropyl ether at flow rates of 10 L/h and 200 L/h, respectively. The slurry was filtered and the filter cake was dried in a vacuum oven at 60°C for 12 h, yielding the powder.

Scanning Electron Microscope Imaging

The powder samples were mounted onto metal sample plates and coated with platinum/gold (50 nm thick). The samples were then examined under a high resolution field emission scanning electron microscope (Jeol JSM 6000F, Japan) at 3 kV.

Primary Particle Size Determination

The primary particle size of the nanoparticles was determined via the dynamic light scattering technique (Malvern Zetasizer 3000 HS, UK) using water as the dispersing medium.

Powder Crystallinity

Powder crystallinity of both the raw material and nanoparticles were assessed by X-ray powder diffraction (XRD). Samples were packed onto a glass sample plate and analyzed on an X-ray powder diffractometer (Siemens D5000, Germany) using CuKα radiation generated at 40 kV and 30 mA, and at an angular increment of 0.04°/s.

Surface Area Determinations

The specific surface area of the powders was determined by a surface area analyzer (Micromeritics Tristar 3000, USA), using nitrogen as the adsorbate gas. Excess moisture was removed from the powders (500 mg) via heating at 50°C for 20 h on a vacuum dryer (Micromeritics Vacprep 061, USA). The specific surface area was then determined by the multipoint Brunauer–Emmett–Teller (BET) gas adsorption/desorption method.

True Density

The true densities of the powders were determined by helium pycnometry (39) (Micromeritics Multivolume Pyc-

nometer 1305, USA) in triplicate. Briefly, an empty sample cup was pre-weighed and approximately 1 g of sample was placed in the cup. The cup was then introduced into the instrument, and the contained sample was purged for 15 min with helium to remove trapped air and vapors before commencement of the test.

Drug Solubility

The saturation solubilities of both species were determined by equilibrating an excess of each species (i.e. 50 mg and 100 mg for the unprocessed and nanosized forms, respectively) in 30 mL dissolution medium (0.1 M HCl, BDH AnalaR, USA) containing 0.1% *w/v* sodium dodecyl sulphate (J.T. Baker Ultrapure Bioreagent, USA) at 37.0± 0.5°C and 500 rpm (Variomag Multipoint-15 magnetic stirrer, Germany) for 5 days. The samples were initially sonicated for 5 min to fully disperse the powders into the fluid. The tubes were sealed for the duration of the test, and equilibrium was determined by repetitive sampling of two milliliter samples filtered through 0.2 μm PTFE syringe filters (Millipore Millex-LG, Japan) and assaying on the UV–Vis spectrophotometer (Hitachi U-2000, Japan) at 278 nm. The studies were carried out in triplicate.

Powder Dissolution

USP Apparatus I (Basket)

Twenty milligram samples were placed into the baskets and introduced into three vessels of the dissolution tester (VanKel VanderKamp VK6000, USA), each containing 900 mL dissolution medium (0.1 M HCl, BDH AnalaR, USA) and 0.1% *w/v* sodium dodecyl sulphate (J.T. Baker Ultrapure Bioreagent, USA). Basket speed and bath temperature were maintained at 100 rpm and 37.0±0.5°C, respectively. Five milliliter samples were withdrawn every 5 min, filtered through a 0.2 μm PTFE syringe filter (Millipore Millex-LG, Japan) and analyzed in a UV–Vis spectrophotometer (Hitachi U-2000, Japan) at 278 nm. Studies were carried out in triplicate.

USP Apparatus II (Paddle)

The procedure was the same as the above except that the 20 mg samples were introduced directly into the vessels without the basket.

USP Apparatus IV (Flow-through cell)

Nine hundred milliliter dissolution medium (0.1 M HCl) containing 0.1% *w/v* sodium dodecyl sulphate at 37.0±0.5°C was passed through a 25 mm i.d. flow-through cell (Millipore Swinnex filter holders, USA, utilizing a Pall HT Tuffryn 0.2 μm membrane disc filters, USA) containing 20 mg of sample, and re-circulated in a closed-loop configuration (34) at 1.6 mL/min using a peristaltic pump (pump speed stability of ±0.5%) (Gilson MiniPuls3, USA). At regular time intervals, 5 mL samples were withdrawn, and their concentrations were analyzed in a UV–Vis spectrophotometer at 278 nm. Studies were carried out in triplicate.

Dialysis

A dialysis bag (molecular weight cut-off 12,000–14,000 Da; Visking, UK) was filled with 20 mg samples and 7 mL dissolution medium (0.1 M HCl) containing 0.1% *w/v* sodium dodecyl sulphate and introduced into three vessels of the dissolution tester, each containing 900 mL of the same dissolution medium. Paddle speed and bath temperature were maintained at 100 rpm and 37.0±0.5°C, respectively. Five milliliter samples were withdrawn and analysed as described above.

Initial Dissolution Rate Ratios

The initial dissolution rate ratios obtained from the different dissolution apparatus were calculated at their first time-points (i.e. ≤5 min into the dissolution process):

$$\frac{\left(\frac{dM}{dt}\right)_{\text{nanoparticles}}}{\left(\frac{dM}{dt}\right)_{\text{unprocessed}}} = \frac{\left(\text{Slope} = \frac{\%\text{Dissolved}}{\text{Time}}\right)_{\text{nanoparticles}}}{\left(\text{Slope} = \frac{\%\text{Dissolved}}{\text{Time}}\right)_{\text{unprocessed}}} \quad (5)$$

RESULTS AND DISCUSSION

As reported previously (12), CFA nanoparticles produced by the High-Gravity Antisolvent Precipitation method were 'chain-like' aggregates (Fig. 1a), with a mean primary

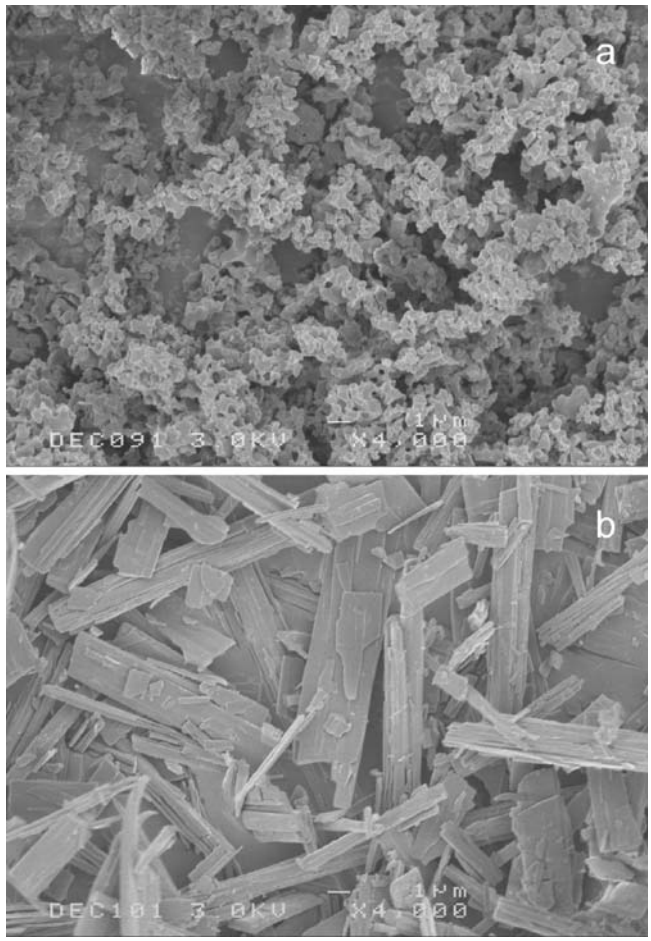

Fig. 1. SEM images of **a** CFA nanoparticles and **b** Unprocessed CFA.

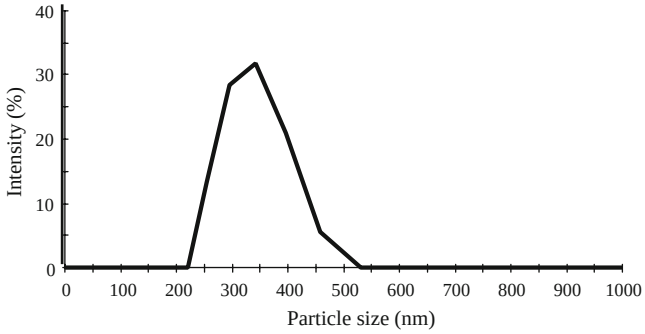

Fig. 2. Primary particle size distribution of CFA nanoparticles.

particle size of about 300 nm (Fig. 2). These particles had a specific surface area of 16.91±0.05 m^2/g, about 2.71 times higher than that (i.e. 6.24±0.03 m^2/g) obtained for the unprocessed form of the drug (Fig. 1b). The gain in specific surface area was lower than expected for the primary particles because they were linked to each other via 'solid bridges'. Results from the XRD analysis showed that the processed CFA nanoparticles were amorphous (Fig. 3a), while their unprocessed form was crystalline (Fig. 3b). True density determinations of the powders via helium pycnometry showed values of 1.43 g/cm^3 and 1.45 g/cm^3 for the nano-sized and unprocessed forms, respectively. The saturation solubility of the nano-sized form was 2.94 times higher than its unprocessed form (i.e. 2.857 mg/mL and 0.973 mg/mL, respectively). Consequently, this gave a Noyes–Whitney model prediction value of 7.97 for the initial dissolution rate ratio between both species (Table I and Eq. 5).

The Noyes–Whitney relationship predicts a direct proportionality between the dissolution rate and the specific surface area of a powder. Hence, for the CFA nanoparticles, a much faster dissolution rate profile should have been observed. However, the dissolution results from the paddle apparatus (Fig. 4) illustrated the contrary, indicating comparable rates initially, and an eventual slow-down for the nano-sized drug. This anomaly (1,21) was attributed to the propensity of nanoparticles to form aggregates (40,41), leading to a reduced surface area and hence, slower

Table I. A Comparison of the Noyes–Whitney-Predicted Initial Dissolution Rate Ratio and the Experimental Values Obtained from the Various Dissolution Apparatus

$\frac{(dM/dt)_{nanoparticles}}{(dM/dt)_{unprocessed}}$			$\frac{(S \cdot C_S)_{nanoparticles}}{(S \cdot C_S)_{unprocessed}}$
Paddle	Basket	Flow-through	(Model Prediction)
1.00±0.21[a]	1.57±0.33[a]	6.95±1.26[a]	7.97

S Surface area as determined by BET adsorption isotherm, C_s saturation solubility, dM/dt initial dissolution rate
[a] Range (n=3)

dissolution rate. Visually, the nanoparticulate powder was found floating on the surface of the dissolution medium (even with the addition of sodium dodecyl sulphate as a wetting agent), despite the true densities of both materials being higher than that of water. The larger particles had much better wetting properties (1,21) and this was reflected in the more uniform dissolution readings for the unprocessed material. The wide variability in dissolution readings for the nanoparticulate species was attributed to the different degree of aggregation and poor wettability due to reduced surface area. For the paddle apparatus, besides showing unacceptable variability, the experimental dissolution rate ratio for both species (i.e. ratio of about 1) falls short of the model-predicted value of 7.97 (Table I).

The dissolution profile for the basket apparatus (Fig. 5) showed that the nanoparticulate powder began with greater dissolution but gradually fell behind the unprocessed form. This profile showed a 'transitional' phenomenon for the nanoparticulate species, indicative of an initial 'forced' wetting by submerging the powder with the basket into the dissolution medium. The wetting problems became obvious when the particles floated up to the surface of the dissolution medium. This was in good agreement to the findings of Nicklasson et al. (23) who noted that the basket method did not generate adequate liquid flow past the surface of the powder particles, hence resulting in the eventual formation of aggregates inside the basket and the associated wetting problems. There was subsequent adherence of the aggregates to the basket walls (23). Similar to the paddle method, there was also considerable variability in dissolution readings for

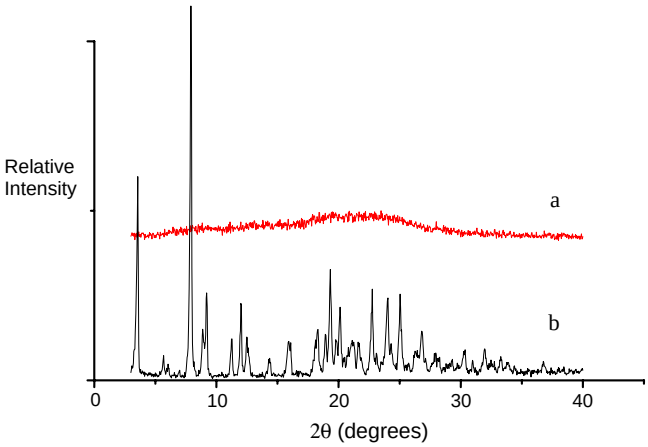

Fig. 3. X-ray diffraction patterns of (*a*) CFA nanoparticles and (*b*) Unprocessed CFA.

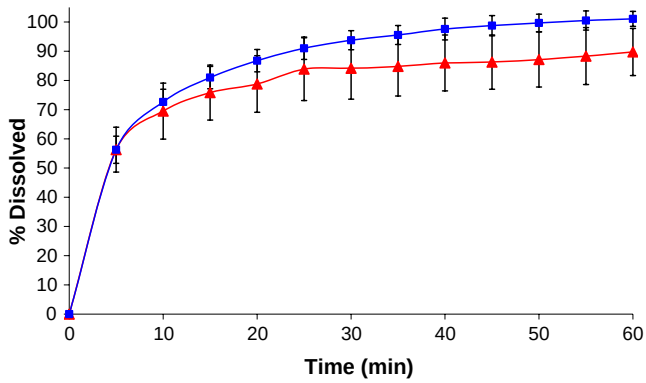

Fig. 4. Dissolution rate profiles obtained from the paddle apparatus (*filled triangles* Nanoparticles, *filled squares* Unprocessed).

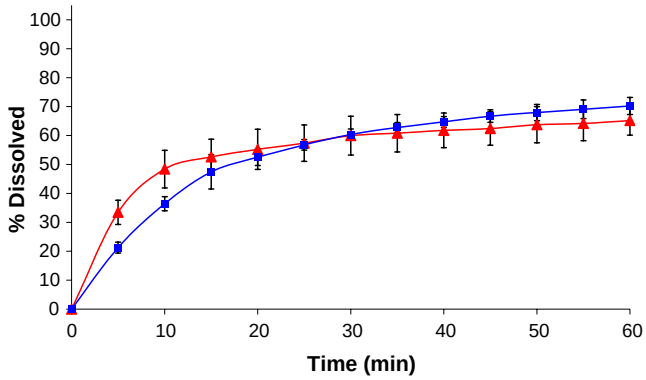

Fig. 5. Dissolution rate profiles obtained from the basket apparatus (*filled triangles* Nanoparticles, *filled squares* Unprocessed).

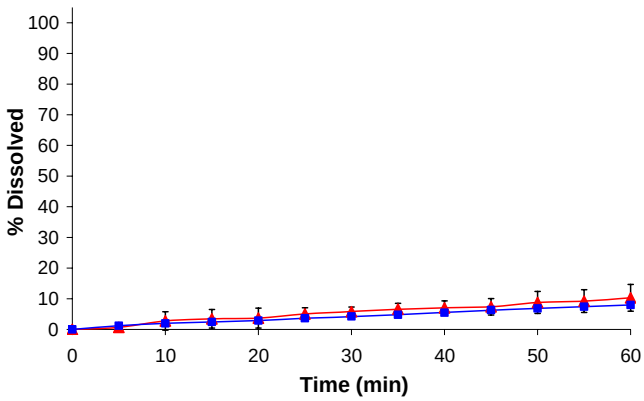

Fig. 7. Dissolution rate profiles obtained from dialysis (*filled triangles* Nanoparticles, *filled squares* Unprocessed).

the nanoparticulate species as a consequence of poor wetting (1,21). Initially, the experimental dissolution rate ratio for both species in the basket (i.e. 1.57; Table I) was poorly approximated to the model-predicted value of 7.97. Hence, it can be concluded that dissolution testing of powders via both the paddle and basket apparatus is inaccurate due to inherent wetting problems (26), and the low initial dissolution rate ratios obtained (Table I) are not representative of the actual powder dissolution.

In the flow-through cell setup, the powder was held in place in the cell, hence minimising any wetting or floating problems. The dissolution profiles (Fig. 6) showed excellent discriminatory behaviour between the samples. It is possible that a different choice of flow rate may bring experimental results closer to the theoretical values (42). A low flow rate was used because the apparatus was known to be more discriminating at lower flow rates (24). Lowering the flow rate further would lead to practical difficulties (e.g. slow run times). There was effective size and solubility discrimination as the nanoparticles clearly displayed an increased rate of dissolution over the unprocessed form as a result of the increased surface area and solubility. There was also less variability in the observed dissolution profiles, which was in close accordance to findings in the literature (23,43). These results thus provide direct evidence for the suitability of the flow-through cell for the analysis of nanoparticle dissolution. In addition, the experimental dissolution rate ratio for both species (i.e. ratio of 6.95) compared favorably to the model-predicted value of 7.97 (Table I), in contrast to the paddle and basket techniques. Exact agreement between the measured and theoretical values is not expected, due to the involvement of other factors such as differences in the shape of the particles and the hydrodynamic conditions.

In the dialysis process, the membrane posed an additional barrier to the dissolution process (i.e. despite the use of a high molecular weight cut-off of 12,000–14,000 Da), hence slowing down the dissolution rates of the powders (Fig. 7). Size discrimination was very modest, as the nanoparticles only displayed a slight increase in the dissolution rate compared with the unprocessed form. In addition, the small percent released suggested that the dialysis process was rate-limited by the membrane rather than the dissolution process itself. This method was therefore not included in the dissolution rate analysis shown in Table I.

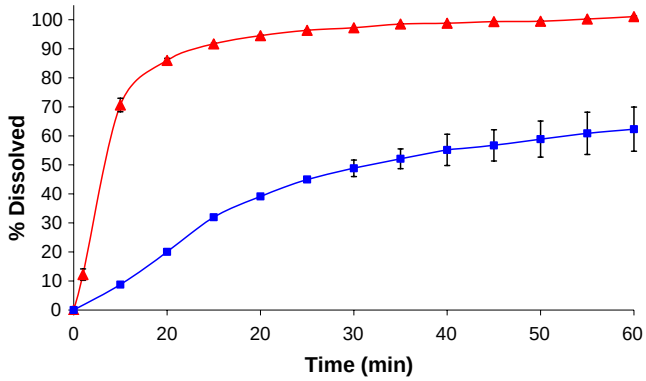

Fig. 6. Dissolution rate profiles obtained from the flow-through cell (*filled triangles* Nanoparticles, *filled squares* Unprocessed).

CONCLUSIONS

In conclusion, the flow-through cell has been shown to be most suitable for dissolution analysis and performance evaluation of drug nanoparticles. Furthermore, this work is the first to show that the dissolution profiles of nanoparticles follow the Noyes–Whitney and similar models. The ability of the flow-through method to discern the true extent of nanoparticle dissolution will be beneficial in the optimization of poorly soluble drugs and study of nanoparticle release rate.

ACKNOWLEDGEMENTS

The authors are grateful to Lee Ford-Griffiths (Particle & Surface Sciences Pty. Ltd.) for the BET analysis and staff of the Electron Microscope Unit (The University of Sydney) for kind usage of the field emission scanning electron microscope and the X-ray powder diffractometer. This work was supported by a grant from the Australian Research Council (ARC Linkage Project LP 0561675 with Nanomaterials Technology Pty. Ltd). One of the authors (JAR) is currently at the National Science Foundation. Any opinion, findings, and conclusions or recommendations expressed in this material are those of the authors and do not necessarily reflect the views of the National Science Foundation.

REFERENCES

1. A. Dokoumetzidis and P. Macheras. A century of dissolution research: from Noyes and Whitney to the biopharmaceutics classification system. *Int. J. Pharm.* **321**:1–11 (2006).
2. B. R. Rohrs. Dissolution method development for poorly soluble compounds. *Dissolution Technologies* **8**:1–5 (2001).
3. G. H. Zhang, W. A. Vadino, T. T. Yang, W. P. Cho, and I. A. Chaudry. Evaluation of the flow-through cell dissolution apparatus: effects of flow rate, glass beads and tablet position on drug release from different types of tablets. *Drug Dev. Ind. Pharm.* **20**:2063–2078 (1994).
4. A. A. Noyes and W. R. Whitney. The rate of solution of solid substances in their own solutions. *J. Am. Chem. Soc.* **19**:930–934 (1897).
5. M. Gibaldi, S. Feldman, R. Wynn, and N. D. Weiner. Dissolution rates in surfactant solutions under stirred and static conditions. *J. Pharm. Sci.* **57**:787–791 (1968).
6. W. I. Higuchi. Diffusional models useful in biopharmaceutics. *J. Pharm. Sci.* **56**:315–324 (1967).
7. P. Veng Pedersen and K. F. Brown. Experimental evaluation of three single-particle dissolution models. *J. Pharm. Sci.* **65**:1442–1447 (1976).
8. B. Y. Shekunov, P. Chattopadhyay, J. Seitzinger, and R. Huff. Nanoparticles of poorly water-soluble drugs prepared by supercritical fluid extraction of emulsions. *Pharm. Res.* **23**:196–204 (2006).
9. M. H. El-Shabouri. Nanoparticles for improving the dissolution and oral bioavailability of spironolactone, a poorly-soluble drug. *STP Pharma Sciences* **12**:97–101 (2002).
10. E. Reverchon and R. Adami. Nanomaterials and supercritical fluids. *J. Supercrit. Fluids* **37**:1–22 (2006).
11. H. Eerikainen, W. Watanabe, E. I. Kauppinen, and P. P. Ahonen. Aerosol flow reactor method for synthesis of drug nanoparticles. *Eur. J. Pharm. Biopharm.* **55**:357–360 (2003).
12. J. F. Chen, J. Y. Zhang, Z. G. Shen, J. Zhong, and J. Yun. Preparation and characterisation of amorphous cefuroxime axetil drug nanoparticles with novel technology: high-gravity antisolvent precipitation. *Ind. Eng. Chem. Res.* **45**:8723–8727 (2006).
13. M. A. Lopez-Quintela. Synthesis of nanomaterials in microemulsions: formation mechanisms and growth control. *Curr. Opin. Colloid Interface Sci.* **8**:137–144 (2003).
14. B. K. Johnson and R. K. Prud'homme. Chemical processing and micromixing in confined impinging jets. *Alchem. J.* **49**:2264–2282 (2003).
15. R. H. Muller and J. A. H. Junghanns. Drug nanocrystals/nanosuspensions for the delivery of poorly soluble drugs. In V. P. Torchilin (ed.), *Nanoparticulates as Drug Carriers*, Imperial College Press, London, 2006, pp. 308–309.
16. R. B. Gupta. Fundamentals of drug nanoparticles. In R. B. Gupta, and U. B. Kompella (eds.), *Drugs and the Pharmaceutical Sciences: Nanoparticle Technology for Drug Delivery*, Taylor and Francis, New York, 2006, pp. 6–9.
17. L. M. Katz. Nanotechnology and applications in cosmetics: general overview. *American Chemical Society Symposium Series (2007)* **961**:193–200 (2007).
18. C. A. Lipinski, F. Lombardo, B. W. Dominy, and P. J. Feeney. Experimental and computational approaches to estimate solubility and permeability in drug discovery and development settings. *Adv. Drug Deliv. Rev.* **23**:3–25 (1997).
19. I. Kanfer. Report on the international workshop on the biopharmaceutics classification system (BCS): scientific and regulatory aspects in practice. *J. Pharm. Pharm. Sci.* **5**:1–4 (2002).
20. N. Rasenack, H. Hartenhauer, and B. W. Muller. Microcrystals for dissolution rate enhancement of poorly water-soluble drugs. *Int. J. Pharm.* **254**:137–145 (2003).
21. P. Finholt. Influence of formulation on dissolution rate. In L. J. Leeson, and J. T. Carstensen (eds.), *Dissolution Technology*, The Industrial Pharmaceutical Technology Section of the Academy of Pharmaceutical Science, Washington, 1974, pp. 106–146.
22. E. Leo, R. Cameroni, and F. Forni. Dynamic dialysis for the drug release evaluation from doxorubicin–gelatin nanoparticle conjugates. *Int. J. Pharm.* **180**:23–30 (1999).
23. M. Nicklasson, A. Orbe, J. Lindberg, B. Borga, A. B. Magnusson, G. Nilsson, R. Ahlgren, and L. Jacobsen. A collaborative study of the *in vitro* dissolution of phenacetin crystals comparing the flow through method with the USP paddle method. *Int. J. Pharm.* **69**:255–264 (1991).
24. B. Wennergren, J. Lindberg, M. Nicklasson, G. Nilsson, G. Nyberg, R. Ahlgren, C. Persson, and B. Palm. A collaborative *in vitro* dissolution study: comparing the flow-through method with the USP paddle method using USP prednisone calibrator tablets. *Int. J. Pharm.* **53**:35–41 (1989).
25. K. Gjellan, A. B. Magnusson, R. Ahlgren, K. Callmer, D. F. Christensen, U. Espmarker, L. Jacobsen, K. Jarring, G. Lundin, G. Nilsson, and J. O. Waltersson. A collaborative study of the *in vitro* dissolution of acetylsalicylic acid gastro-resistant capsules comparing the flow-through cell method with the USP paddle method. *Int. J. Pharm.* **151**:81–90 (1997).
26. H. Moller. Dissolution testing of different dosage forms using the flow-through method. *Pharm. Ind.* **45**:617–622 (1983).
27. H. Moller and E. Wirbitzki. Special cases of dissolution testing using the flow-through system. *STP Pharma Sciences* **6**:657–662 (1990).
28. F. Langenbucher, D. Benz, W. Kurth, H. Moller, and M. Otz. Standardized flow-cell method as an alternative to existing pharmacopoeial dissolution testing. *Pharm. Ind.* **51**:1276–1281 (1989).
29. A. D. Karande and P. G. Yeole. Comparative assessment of different dissolution apparatus for floating drug delivery systems. *Dissolution Technologies* **13**:20–23 (2006).
30. M. C. Gohel, P. R. Mehta, R. K. Dave, and N. H. Bariya. A more relevant dissolution method for evaluation of floating drug delivery system. *Dissolution Technologies* **11**:22–25 (2004).
31. P. P. Sanghvi, J. S. Nambiar, A. J. Shukla, and C. C. Collins. Comparison of three dissolution devices for evaluating drug release. *Drug Dev. Ind. Pharm.* **20**:961–980 (1994).
32. J. Hu, A. Kyad, V. Ku, P. Zhou, and N. Cauchon. A comparison of dissolution testing on lipid soft gelatin capsules using USP apparatus 2 and apparatus 4. *Dissolution Technologies* **12**:6–9 (2005).
33. E. Beyssac and J. Lavigne. Dissolution study of active pharmaceutical ingredients using the flow through apparatus USP 4. *Dissolution Technologies* **12**:23–25 (2005).
34. S. N. Bhattachar, J. A. Wesley, A. Fioritto, P. J. Martin, and S. R. Babu. Dissolution testing of a poorly soluble compound using the flow-through cell dissolution apparatus. *Int. J. Pharm.* **236**:135–143 (2002).
35. B. A. Hendriksen. Characterization of calcium fenoprofen. 1. Powder dissolution rate and degree of crystallinity. *Int. J. Pharm.* **60**:243–252 (1990).
36. J. Hecq, M. Deleers, D. Fanara, H. Vranckx, and K. Amighi. Preparation and characterization of nanocrystals for solubility and dissolution rate enhancement of nifedipine. *Int. J. Pharm.* **299**:167–177 (2005).
37. J. L. Baxter, J. Kukura, and F. J. Muzzio. Shear-induced variability in the United States pharmacopoeia apparatus 2: modifications to the existing system. *AAPS J.* **7**:E857–E864 (2006).
38. D. H. Adams, M. J. Wood, and I. D. Farrell. Oral cefuroxime axetil: clinical pharmacology and comparative dose studies in urinary tract infection. *J. Antimicrob. Chemother.* **16**:359–366 (1985).
39. Micromeritics. Instruction manual (Multivolume Pycnometer 1305) for determining skeletal density and volume of powders, porous materials, and irregularly shaped solid objects, Micromeritics Instrument Corporation, USA, 1992.
40. D. Horn and J. Rieger. Organic nanoparticles in the aqueous phase—theory, experiment, and use. *Angew. Chem. Int. Ed.* **40**:4330–4361 (2001).
41. A. Tandya, F. Dehghani, and N. R. Foster. Micronisation of cyclosporine using dense gas techniques. *J. Supercrit. Fluids* **37**:272–278 (2006).
42. P. J. Missel, L. E. Stevens, and J. W. Mauger. Reexamination of convective diffusion/drug dissolution in a laminar flow channel: accurate prediction of dissolution rate. *Pharm. Res.* **21**:2300–2306 (2004).
43. M. Nicklasson, B. Wennergren, J. Lindberg, C. Persson, R. Ahlgren, B. Palm, A. Pettersson, and L. Wenngren. A collaborative *in vitro* dissolution study using the flow-through method. *Int. J. Pharm.* **37**:195–202 (1987).